MM Science Journal | www.mmscience.eu
ISSN 1803-1269 (Print) | ISSN 1805-0476 (On-line)
Special Issue | CUTTING TOOLS 2024
1st International Conference on Cutting Tools
November 20-22, 2024, Trnava, Slovakia
DOI: 10.17973/MMSJ.2025_03_2025016

CUTTINGTOOLS2024-00007

GEOMETRIC ANALYSIS AND MATHEMATICAL MODEL OF A POLYCENTRIC KNEE MECHANISM

P. Niznan[1]*, M. Csekei[1], J. Sido[1], P. Kostal[1], R. Zelnik[1]
[1]Slovak University of Technology in Bratislava, Faculty of Materials Science and Technology in Trnava, Institute of Production Technologies, Trnava, Slovakia
*peter.niznan@stuba.sk

Abstract
This paper focuses on calculating the central distances of polycentric joints designed to replicate the natural motion of the human knee. A key aspect is the shortening of the central distance during the swing phase, which reduces tripping risk and improves gait stability. Using mathematical modeling, the study analyzes the dynamic changes in instantaneous centers of rotation and their impact on knee biomechanics. The results enable a more precise design of polycentric prosthetic joints, enhancing their functionality and adaptability for users.

Keywords:
Polycentric, Joint, Ellipse, Knee, Prothesis

1 INTRODUCTION

The human knee is one of the most complex joints in the human body, playing a crucial role not only in movement but also in stabilizing the body in various static and dynamic situations. Its unique anatomy allows for a wide range of movements while providing the necessary stability for daily activities and physically demanding tasks. The knee connects the femur, tibia, and patella, allowing not only flexion and extension but also lateral and rotational movements essential for a natural gait pattern. [Dupes 2004; Gottschalk 1999]

Unlike simple joints with a fixed axis of rotation, the knee exhibits polycentric motion, meaning that its instantaneous centers of rotation shift dynamically throughout movement. This variability results from complex interactions between anatomical structures such as ligaments, muscles, joint surfaces, and synovial fluid. Thanks to this mechanism, the knee effectively adapts to various external conditions and biomechanical demands, ensuring stability even on uneven terrain or during sudden movement changes. [Bolcos 2018; Heller 2007; Ralfs 2023]

One of the key characteristics of knee movement is its ability to shorten the effective length of the lower limb during the swing phase of walking. This process enables the leg to pass over obstacles smoothly while minimizing the risk of tripping. Additionally, the dynamic adaptation of rotation centers helps distribute mechanical stress evenly across surrounding tissues, reducing the likelihood of cartilage wear and premature joint degeneration. [Dupes 2004; Shi 2024]

Replicating these complex biomechanical properties within prosthetic systems is a significant challenge. Traditional prosthetic knee joints often rely on simple mechanisms with fixed rotation axes, resulting in unnatural movement patterns and increased energy expenditure during walking. Polycentric knee joints offer a promising solution by allowing dynamic changes in central distance, closely mimicking the natural biomechanics of the knee. [Buckley 1997; Carney 2021; Hsiao-Wecksler 2010; Legro 1998; Perry 2004]

This study focuses on designing a polycentric joint that accurately replicates the natural shortening of central distance observed in the human knee. Using mathematical modeling, various design parameters influencing joint movement are analyzed to develop a system that is efficient, stable, and energy efficient. This approach not only enhances prosthetic functionality but also improves user adaptability across different movement scenarios. [Bellmann 2020; Kistenberg 2014; Shi 2024]

The following sections of this article detail the methodology for designing the polycentric joint, with particular emphasis on calculating instantaneous centers of rotation. The goal is to provide new insights into modern prosthetic technology development and bring the design of artificial joints closer to the natural movement patterns of a healthy human knee. [Anand 2017; Hsiao-Wecksler 2010]

2 METHODS

The polycentric joint was designed to mimic the natural movement of the human knee, with the primary objective of shortening the central distance during motion. This type of joint utilizes a combination of elliptical and circular

components, allowing for controlled rolling motion between the individual segments (Tab. 1).

Tab. 1 : Joint types based on shape combinations

RXR	AvBXAvB	AmBXAmB	RXAvB	RXAmB	AvBXAmB
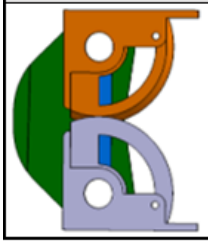	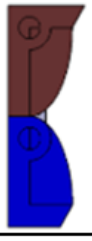	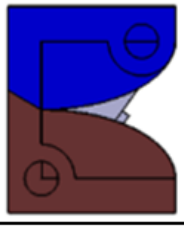	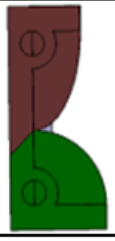	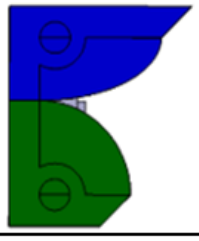	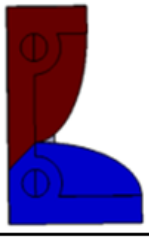

When designing a polycentric joint, it is crucial to consider different shape combinations and their interactions. When two circular components are used, the calculation is significantly simplified, as the radii of both components allow for identical rolling motion. On the other hand, if elliptical components are used, it is essential to precisely define the major and minor axes of each ellipse to prevent incorrect rolling distance calculations. The composition of these parts, together with the mathematical model, aims to create a joint that replicates the movement of a real human knee through adjustments.

A significant aspect of the design is determining the final rotation angle of the polycentric joint. This angle depends on the contact points between the individual components and their ability to maintain a consistent rolling distance value. If this equality is achieved, it becomes possible to establish accurate values for the joint's rotation and, consequently, its overall kinematics.

In the graphical representation of the design, circular components are labeled as "R" while elliptical components are categorized based on their contact axis. If they contact the other part of the joint along their major axis, they are labeled as AvB, and if they contact along their minor axis, they are labeled as AmB. Specific component combinations are represented by the symbol X, with an example of such a combination being RXAvB.

2.1 Work plan

To achieve the set goals, a work plan (Fig. 1) was developed, which describes the individual steps necessary to achieve the expected results.

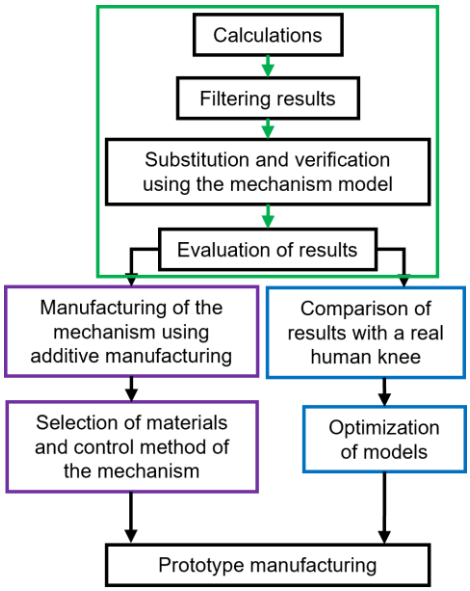

Fig. 1: Work plan

This plan includes not only theoretical analysis but also practical steps that will lead to the implementation of the polycentric joint, which will most accurately replicate the movements of the human knee. The portion marked in green highlights the steps that describe the evaluation process of the proposed models, and the preparation needed to create a functional mechanism.

After the initial design of the models, calculations were performed, and their results were subsequently verified using existing mechanism models. These results were analyzed and summarized in a table. The further course of work is elaborated in Fig. 1 and in Chapter 4.1 *Further work*.

2.2 Calculations

For each of these combinations, the differences in central distance during bending were subsequently calculated. The flexion values of the joint were set from 0 to 150 degrees. The radius of the circular components was denoted as R, and the rotation angle as α. The formula (1) used to calculate the length l_c of the rolling arc was as follows:

$$l_c = \frac{\alpha * \pi * R}{180} \text{ [mm]} \quad (1)$$

For the ellipses, the lengths of the major and minor semi-axes were denoted as A and B, respectively. The angles formed with the center during the rolling of the ellipses were labeled β and γ. If the semi-axis A was larger than the semi-axis B, A was considered the major semi-axis. Conversely, if A was smaller, it was treated as the minor semi-axis. The formulas used to calculate the lengths l_1 (2) and l_2 (3) of the rolling arcs were as follows:

$$l_1 = \int_0^{\beta} \sqrt{A^2 * \sin(t)^2 + B^2 * \cos(t)^2}\, dt \text{ [mm]} \quad (2)$$

$$l_2 = \int_0^{\gamma} \sqrt{B^2 * \sin(f)^2 + A^2 * \cos(f)^2}\, df \text{ [mm]} \quad (3)$$

l_1 represents the arc length of an ellipse where A is the major semi-axis and B is the minor semi-axis. The arc length l_2 corresponds to the ellipse where A is the minor semi-axis. The angles β and γ are the angles formed by the rotation along the ellipse, starting from the vertex of the major semi-axis.

During rotation by a certain angle, it is necessary to define where the rotation angle is located. In the case of both circular components and ellipses, the angle is subtended between the minor semi-axis and the tangent to the ellipse. The angles of the tangents are denoted as δ and ε. The formulas (4), (5) used to calculate the angles of the tangents are as follows:

$$\tan \delta = \frac{B * \cot(\beta)}{-A} \quad (4)$$

$$\tan \varepsilon = \frac{A * \cot(\gamma)}{-B} \quad (5)$$

The distance from the base lying on the major semi-axis to the point of contact is calculated using the following formulas (6), (7):

$$x_1 = A * \cos(\beta) \text{ [mm]} \quad (6)$$

$$x_2 = B * \cos(\gamma) \text{ [mm]} \quad (7)$$

For calculating the distance for a circle x_R, the following formula (8) was used:

$$x_R = R * \cos(\alpha) \text{ [mm]} \quad (8)$$

To calculate the difference in central distance within the joint, it is necessary to define the joint rotation angle τ. In cases where the ellipses are oriented identically, the following formulas (9), (10) can be used:

$$\tau = 2\delta \text{ [°]} \quad (9)$$

$$\tau = 2\varepsilon \text{ [°]} \quad (10)$$

If it is a combination of an ellipse and a circle, or if the ellipses are not identically rotated, the formulas (11-13) for the resulting rotation angle in the joint will have the condition of equality of the lengths of the rolled arcs along the ellipse or circle:

$$\tau = \delta + \varepsilon \quad \cap \quad l_1 = l_2 \quad (11)$$

$$\tau = \delta + \alpha \quad \cap \quad l_1 = l_R \quad (12)$$

$$\tau = \varepsilon + \alpha \quad \cap \quad l_2 = l_R \quad (13)$$

The results included data pairs of lengths l_c, l_1, l_2, traversed along the ellipse or circle in the given mechanism, the angles α,β,γ formed in the ellipse or circle, and the coordinates X,Y of the contact points for the individual ellipses or circles, which were used to calculate the resulting difference in central distance. All these values were computed for each angle τ in the mechanism within the range of 0° to 150°.

System of equations for RXAvB

A system of equations (14), (15) was used to calculate the difference in central distance:

$$\tau = 90 - \alpha + \tan^{-1}\left(\frac{B*\cot\beta}{-A}\right) \quad (14)$$

$$\frac{\alpha*\pi*R}{180} = \int_0^{\beta} \sqrt{A^2 * \sin(t)^2 + B^2 * \cos(t)^2}\, dt \quad (15)$$

Subsequently, the angles α and β are isolated from the equations. Using these angles, the coordinates on the X-axis are calculated (16), (17). These coordinates represent the distance from the base to the contact point. After subtracting from the original value, the difference in central distance D_c is obtained:

$$D_c = (R - x_R) + (A - x_1) \text{ [mm]} \quad (16)$$

$$D_c = (R - R * \cos\alpha) + (A - A * \cos\beta) \text{ [mm]} \quad (17)$$

System of equations for RXAmB

Similarly to the mechanism RxAvB, a system of equations (18), (19) was used, where the equations of the ellipses are replaced with equations defined for an ellipse where the major axis is shorter.

$$\tau = 90 - \alpha + \tan^{-1}\left(\frac{A*\cot\gamma}{-B}\right) \quad (18)$$

$$\frac{\alpha*\pi*R}{180} = \int_0^{\gamma} \sqrt{B^2 * \sin(f)^2 + A^2 * \cos(f)^2}\, df \quad (19)$$

The angles α and γ are isolated from the equations. Using the obtained angles, the coordinates are calculated and the difference in the joint's central distance is determined:

$$D_c = (R - x_R) + (B - x_2) \text{ [mm]} \quad (20)$$

$$D_c = (R - R * \cos\alpha) + (B - B * \cos\gamma) \text{ [mm]} \quad (21)$$

System of equations for AvBXAmB

To calculate the difference in central distance for the mechanism AvBXAmB, a system of equations (22), (23) was used:

$$\tau = \tan^{-1}\left(\frac{B*\cot\beta}{-A}\right) + \tan^{-1}\left(\frac{A*\cot\gamma}{-B}\right) \quad (22)$$

$$\int_0^{\beta} \sqrt{A^2 * \sin(t)^2 + B^2 * \cos(t)^2}\, dt = \int_0^{\gamma} \sqrt{B^2 * \sin(f)^2 + A^2 * \cos(f)^2}\, df \quad (23)$$

To calculate the difference in central distance, the angles β and γ were isolated. They were then substituted into equations (24), (25), and the difference in central distance was determined:

$$D_c = (A - x_1) + (B - x_2) \text{ [mm]} \quad (24)$$

$$D_c = (A - A * \cos\beta) + (B - B * \cos\gamma) \text{ [mm]} \quad (25)$$

After creating and defining the equations, it is possible to proceed with the calculations, whose results will then be evaluated.

System of equations for RXR, AvBXAvB, AmBXAmB

For shape combinations that touch with identical elements, such as the same radius or the same semi-axis, the calculation is simplified, as the equality of the rolling distance is automatically preserved. The result of the difference in central distance is therefore calculated using formulas (26) for a circle, where in the calculation of x_R, the angle α can be replaced by $\tau/2$:

$$D_c = (2R - 2x_R) \text{ [mm]} \quad (26)$$

For ellipses, the formula for the central distance will be in the form :

$$D_c = (2A - 2x_1) \text{ [mm]} \quad (27)$$

For ellipses where B is the major semi-axis, and

$$D_c = (2B - 2x_2) \text{ [mm]} \quad (28)$$

For ellipses where B is the major semi-axis.

The equations (9) and (10) for tangent angles were used.

3 RESULTS AND DISCUSION

The calculations were created in MATLAB R2024b. The results were exported to tables. As an example in Tab. 2 is D_R defined as difference of central distance in circle and D_β as difference of central distance in ellipse AvB.

Tab 2 : Results of calculations from MATLAB for RXAvB

τ	α	β	l_R	l_1	x_R	x_1	D_R	D_β	D_c
1	0,2500	0,7499	0,0654	0,0654	14,9998	19,7382	0,0002	0,2617	0,2619
2	0,5000	1,4999	0,1309	0,1309	14,9995	19,4764	0,0005	0,5235	0,5240
…									
149	68,4003	80,5996	17,9072	17,9072	5,5218	0,2686	9,4782	19,7314	29,2096
150	69,1048	80,8951	18,0916	18,0916	5,3499	0,2520	9,6501	19,7480	29,3981

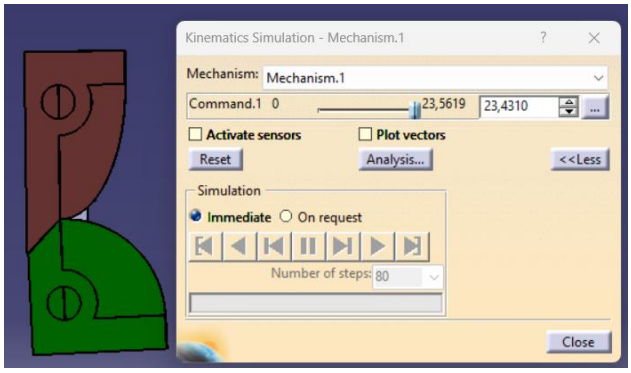

Fig. 2: Entering calculated value in RXAvB mechanism

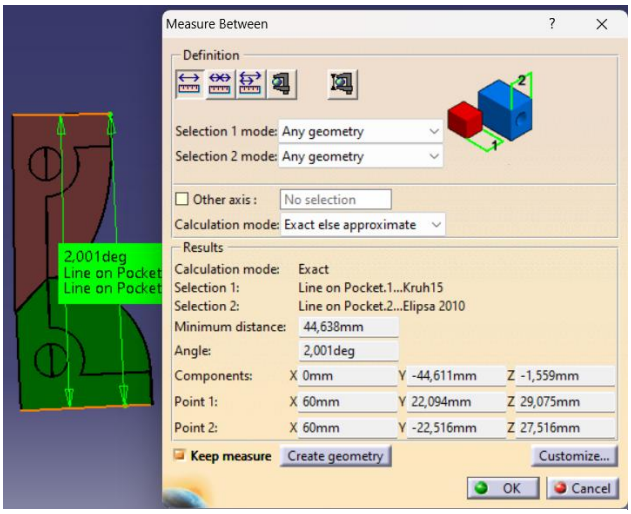

Fig. 3: Measurement of angle in RXAvB mechanism

3.1 Verification of results

To verify the correctness of the calculations, the resulting values were input into mechanisms created in CATIA V5 software, which allows for precise simulation of mechanical systems. In this environment, the rolling distances along elliptical and circular trajectories were defined, with the rolling value l specified in the mechanism. The maximum value at the fully extended joint was 23.5619, and to achieve the desired bending angle, the value l_R needed to be subtracted. After entering the resulting value (Fig. 2), the actual bending angle of the joint was verified using the measurement function in the software (Fig. 3), confirming the accuracy of the calculations.

3.2 Evaluation of results

To quantify the changes in central distance between the components of the polycentric joint, analytical equations were applied to precisely calculate the distance between the base of the joint and the contact point of the components, considering both parts of the mechanism – elliptical and circular. These calculations provided values that were then compared to the original value obtained at full extension of the joint. This approach allowed us to determine the extent to which the central distance was shortened during flexion, which is crucial for understanding changes in the joint's kinematics during movement.

The results of the calculations showed that different combinations of component shapes and their mutual orientation resulted in distinct shortening curves of the central distance.

For all these configurations, which involved various shapes and orientations of components, detailed calculations of central distances were carried out. These calculations were performed within a bending range from 0° to 150°, providing a detailed overview of how the joint behaves during different phases of movement. In this way, we obtained detailed data on the dynamic changes occurring within the joint during movement, which are essential for further development and improvement of this type of mechanism.

The input parameters for the elliptical components were defined as A = 10 mm and B = 20 mm. These values were found to be suitable for representing the standard shape of an ellipse in the context of polycentric joints. For circular trajectories, a radius of R = 15 mm was chosen, which proved to be optimal for this type of kinematic movement. After substituting these parameters into the analytical equations, we obtained specific values, which were then

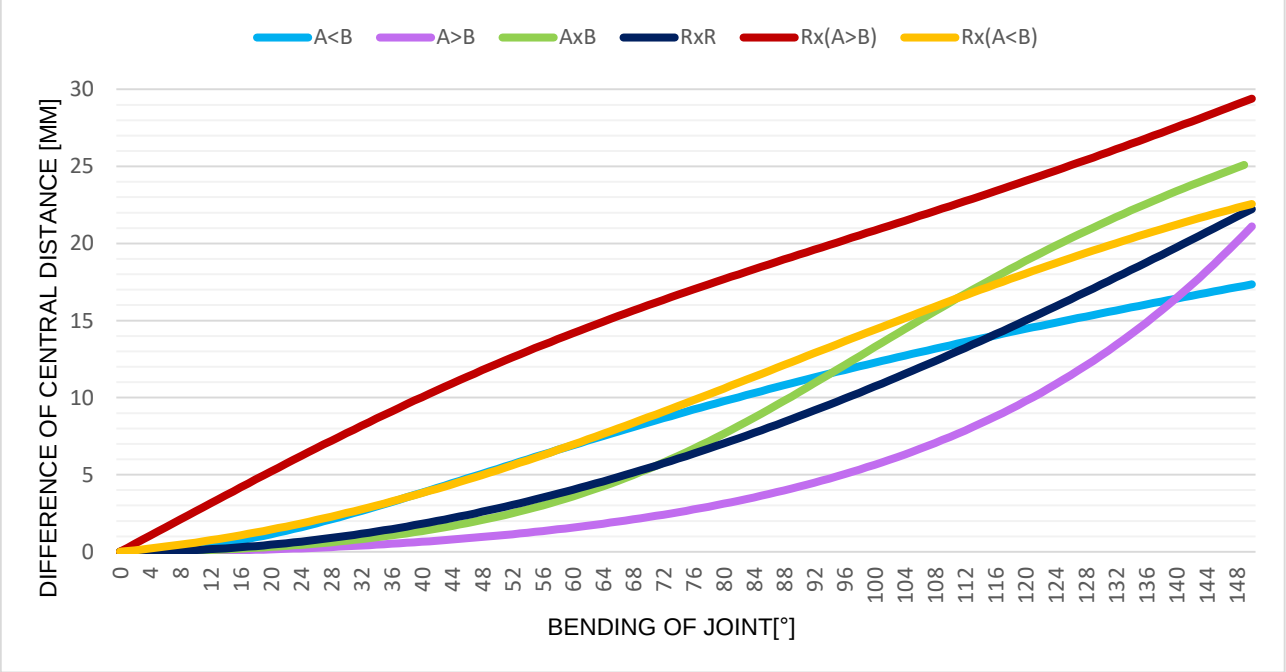

Fig. 4: Difference of central distance in joints with circular and ellipse components

analyzed and visualized in the graph shown in Fig. 4. This graph provided us with an image of the motion characteristics, allowing us to better understand the behavior of the joint during various stages of bending and rotation.

3.3 Application and discussion

The selected parameters represent the curves of central distance shortening, and these curves can be modified by adjusting individual system parameters. Their shape and behavior are directly influenced by the geometry of the elliptical profiles used and the mutual arrangement of kinematic constraints within the mechanism. The possibilities for modification, therefore, depend on the precise configuration of axis lengths, the relative orientation of ellipses, and other structural factors.

The required modifications will be carried out based on a detailed comparison with the shortening curves of a real human knee. For this purpose, available biomechanical data and experimental measurements of real knee joints will be analyzed. Detailed models of real human knee joints will be utilized for further research (Fig. 5), enabling more

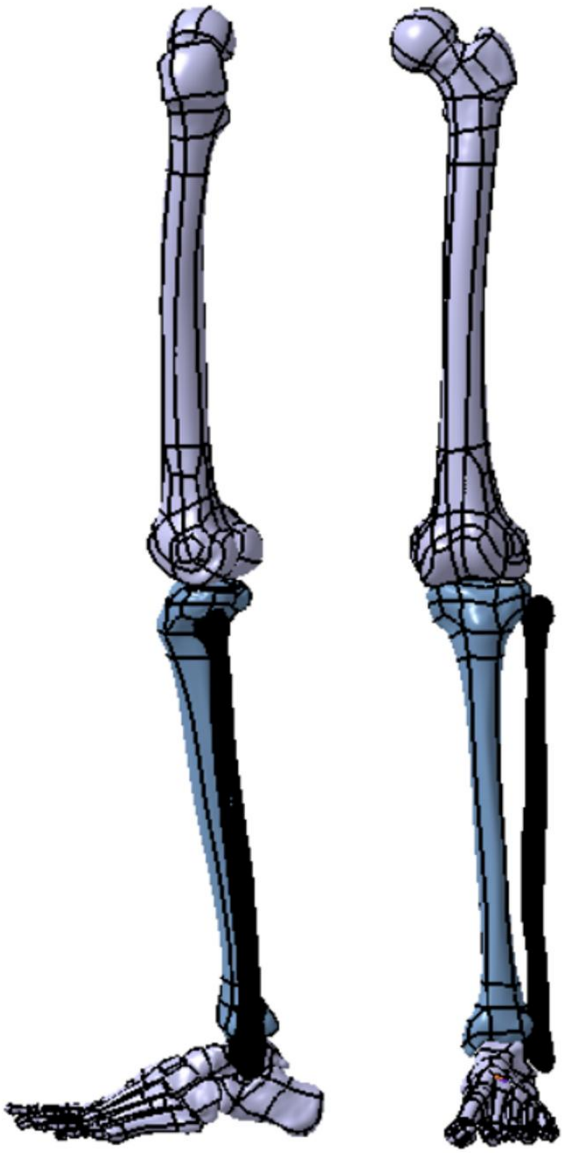

Fig. 5: Model of human lower limb

accurate simulation of their motion. Simulation, combined with experimental measurements, will provide actual shortening curves of the central distance within the joint, allowing verification of the accuracy of the computational models of the mechanism.

The comparison will include a detailed analysis of the calculated mechanism curve shapes against the curve obtained from a real human knee. Based on this analysis, the most suitable combination of shapes for the polycentric mechanism will be identified, with the goal of achieving the best possible match with the natural movement of the knee joint. Once the optimal configuration is selected, the parameters of the individual parts of the mechanism will be adjusted accordingly to ensure that the resulting bending curve closely resembles that of a real human knee.

The knee joint itself is unique to each individual, meaning that its motion characteristics may exhibit individual variations. Therefore, it is essential to first compare the calculated curves with experimentally obtained data from real human knees. This process will enable a more precise optimization of the polycentric mechanism design, ensuring that the final parameters reflect not only theoretical calculations but also the actual biomechanical properties of the human knee.

3.4 Further research

The current mechanism design will be manufactured using additive manufacturing, with the simplest RXR variant selected for initial testing. This configuration will allow for the verification of the basic principles of the mechanism's functionality and behavior under real conditions. The use of additive manufacturing provides flexibility in prototype production, enabling quick modifications and optimizations of the geometry of individual components based on the results of experiments.

The printed components will include elements that were not originally displayed in the conceptual models. These additional parts are essential to ensure the full functionality of the mechanism and its testability. Among the most important modifications are the integration of guiding components, which will serve to properly direct the cables controlling the mechanism's movement. Proper guidance of these cables is crucial for smooth and accurate control of the moving segments of the mechanism.

The cables will be firmly attached to one part of the mechanism and connected to motors on the other side. These motors will regulate the movement of the entire system by winding and unwinding the cables. This control method will enable precise control over the individual segments and will be used to simulate the real biomechanical properties of movement. Additionally, it will allow testing of various control strategies and tuning of parameters for optimal operation of the mechanism.

The entire experiment will serve to verify the functionality of the real model in conditions close to real-world use. Based on the results of these tests, appropriate materials and manufacturing methods for the final prototype will be selected. Furthermore, based on the collected data, the most suitable control system will be determined to ensure precise and reliable control of the mechanism in its future practical application.

4 CONCLUSION

The resulting curves, as well as the values of the central distance obtained from the calculations, are final for the given input parameters and represent the definitive result for the selected configuration. The shape and behavior of these curves depend on the geometric properties of the ellipses that form the mechanism. In the case of a combination of two ellipses, the resulting trajectories will change if the ellipses do not have identical major and minor

axis parameters. Deviations in the ratio of axis lengths can lead to significant changes in the kinematic properties of the mechanism, potentially affecting its functionality and its ability to achieve the desired range of motion.

To ensure the required bending angle of 150 degrees, it is therefore necessary to determine the maximum allowable ratio of the major and minor axis lengths. This ratio should be defined to guarantee smooth and predictable behavior of the mechanism throughout the entire range of motion, without unwanted trajectory deformations or mechanical system constraints.

5 ACKNOWLEDGMENTS

The paper is a part of the research done within the project VEGA 1/0391/24 “Research and Development of a Methodology for Sensor Calibration in Diagnostic Devices for Automated and Robotic Systems” funded by the Slovak Research and Development Agency.

The paper is a part of the research done within the project APVV-23-0084 “Robotic-Based Hybrid Manufacturing of Workpiece for the Concept of Smart Production” funded by the Slovak Research and Development Agency.

6 REFERENCES

[Anand 2017] Anand, T. S., and Sujatha, S. A method for performance comparison of polycentric knees and its application to the design of a knee for developing countries. Prosthetics and Orthotics International, 2017, vol. 41(4), pp. 402–411. doi: 10.1177/0309364616652017

[Bellmann 2020] Bellmann, M., Blumentritt, S., and Köhler, T. M. Polycentric exoprosthetic knee joints - Extent of shortening during swing phase. Canadian Prosthetics and Orthotics Journal, 2020, vol. 3(1), pp. 1–9. doi: 10.33137/cpoj.v3i1.33768

[Bolcos 2018] Bolcos, P. O., Mononen, M. E., Mohammadi, A., Ebrahimi, M., Tanaka, M. S., Samaan, M. A., … Korhonen, R. K. Comparison between kinetic and kinetic-kinematic driven knee joint finite element models. Scientific Reports, 2018, vol. 8(1), pp. 1–11. doi: 10.1038/s41598-018-35628-5

[Buckley 1997] Buckley, J. G., Spence, W. D., and Solomonidis, S. E. Energy cost of walking: Comparison of “intelligent prosthesis” with conventional mechanism. Archives of Physical Medicine and Rehabilitation, 1997, vol. 78(3), pp. 330–333. doi: 10.1016/S0003-9993(97)90044-7

[Carney 2021] Carney, M. E., Shu, T., Stolyarov, R., Duval, J.-F., and Herr, H. M. Design and Preliminary Results of a Reaction Force Series Elastic Actuator for Bionic Knee and Ankle Prostheses. IEEE Transactions on Medical Robotics and Bionics, 2021, vol. 3(3), pp. 542–553. doi: 10.1109/tmrb.2021.3098921

[Dupes 2004] Dupes, B. Prosthetic Knee Systems. Amputee Coalition of America in Partnership with the U.S. Army Amputee Patient Care Program, 2004, vol. 14(1), pp. 1–4. Retrieved from https://www.amputee-coalition.org/resources/prosthetic-knee-systems/

[Gottschalk 1999] Gottschalk, F. Transfemoral Amputation. Clinical Orthopaedics and Related Research, 1999, vol. 361(361), pp. 15–22. doi: 10.1097/00003086-199904000-00003

[Heller 2007] Heller, M. O., König, C., Graichen, H., Hinterwimmer, S., Ehrig, R. M., Duda, G. N., and Taylor, W. R. A new model to predict in vivo human knee kinematics under physiological-like muscle activation. Journal of Biomechanics, 2007, vol. 40 (SUPPL. 1). doi: 10.1016/j.jbiomech.2007.03.005

[Hsiao-Wecksler 2010] Hsiao-Wecksler, E. T., Polk, J. D., Rosengren, K. S., Sosnoff, J. J., and Hong, S. A review of new analytic techniques for quantifying symmetry in locomotion. Symmetry, 2010, vol. 2(2), pp. 1135–1155. doi: 10.3390/sym2021135

[Kistenberg 2014] Kistenberg, R. S. Prosthetic choices for people with leg and arm amputations. Physical Medicine and Rehabilitation Clinics of North America, 2014, vol. 25(1), pp. 93–115. doi: 10.1016/j.pmr.2013.10.001

[Legro 1998] Legro, M. W., Reiber, G. D., Smith, D. G., Del Aguila, M., Larsen, J., and Boone, D. Prosthesis evaluation questionnaire for persons with lower limb amputations: Assessing prosthesis-related quality of life. Archives of Physical Medicine and Rehabilitation, 1998, vol. 79(8), pp. 931–938. doi: 10.1016/S0003-9993(98)90090-9

[Perry 2004] Perry, J., Burnfield, J. M., Newsam, C. J., and Conley, P. Energy expenditure and gait characteristics of a bilateral amputee walking with C-leg prostheses compared with stubby and conventional articulating prostheses. Archives of Physical Medicine and Rehabilitation, 2004, vol. 85(10), pp. 1711–1717. doi: 10.1016/j.apmr.2004.02.028

[Ralfs 2023] Ralfs, L., Hoffmann, N., Glitsch, U., Heinrich, K., Johns, J., and Weidner, R. Insights into evaluating and using industrial exoskeletons: Summary report, guideline, and lessons learned from the interdisciplinary project “Exo@Work.” International Journal of Industrial Ergonomics, 2023, vol. 97 (July). doi: 10.1016/j.ergon.2023.103494

[Shi 2024] Shi, B., Barzan, M., Nasseri, A., Maharaj, J. N., Diamond, L. E., and Saxby, D. J. Automatic generation of knee kinematic models from medical imaging. Computer Methods and Programs in Biomedicine, 2024, vol. 256(April), pp. 108370. doi: 10.1016/j.cmpb.2024.108370